2016 International Symposium on Nonlinear Theory and Its Applications,
NOLTA2016, Yugawara, Japan, November 27th-30th, 2016

Bifurcation Analysis for Early Afterdepolarization in Shannon Model

Ai Takahashi, Hiroyuki Kitajima and Toru Yazawa

†Faculty of Engineering, Kagawa University
2217-20, Hayashi, Takamatsu, Kagawa 761-0396, Japan
Email: s15g472@stu.kagawa-u.ac.jp, {kitaji,tyazawa}@eng.kagawa-u.ac.jp

Abstract—The membrane potential of the ventricular myocyte is regulated through inward and outward ionic currents. When these electrical activities are disturbed, arrhythmia occurs. In particular, QT prolongation is considered to be a sign of sudden cardiac cessation. In this study, we investigate the relationship between the conductivities of ionic currents and the occurrence of such arrhythmias. We obtain that QT prolongation relates to the conductivities of the sodium-calcium exchange current and the L-type calcium current.

1. Introduction

Electrical activities are happening in the cell membrane of myocardial cells. This will serve to regularly contract the heart. The electrical activity is caused by the action potential. A diagram of a typical cardiac action potential is shown in Fig. 1. The action potential refers to the excitement reaction of the cells with depolarization. After the membrane potential is depolarized (approaching 0 [mV]), the action potential occurs when it reaches the threshold membrane potential. The cardiac action potential is categorized into 5 phases : phase 0 (depolarization), phase 1 (spike), phase 2 (plateau), phase 3 (repolarization) and phase 4 (resting potential). When these electrical activities are disturbed, arrhythmia occurs. One of such disturbance is as follows: Usually the membrane potential of the cardiac cell is maintained deep (−90 [mV]). However, if the channel is damaged for any reason, it is difficult to maintain the deep membrane potential. The membrane potential becomes shallow such as −40 [mV]. If the membrane potential is shallow, the potential is staggering. Then it becomes the cause of abnormal electrical activities.

Among abnormal electrical activities of the cardiac cell, here we pay attention to long QT syndrome (LQTS). LQTS is a phenomenon that produces polymorphic ventricular tachycardia so called torsades de pointes (TdP) and prolonged QT interval in the electrocardiogram. LQTS is related to early afterdepolarizations (EADs). LQTS may lead to sudden cardiac cessation due to ventricular fibrillation. Inherited LQTS is classified into 13 types [1]. The most common ones are LQT 1, 2, and 3. It is said that LQT 1 and 2, and 3 are caused by abnormality of calcium and sodium ion channels, respectively [2, 3, 4, 5]. Recently, a novel and selective inhibitor (SEA0400) of the sodium-calcium exchanger (NCX) was detected [6] and its effect on generating LQTS has been studied [7, 8, 9, 10]. Moreover, using the slow-fast analysis, it was shown that an EAD is caused by Hopf and homoclinic bifurcations in the Luo-Rudy I (LRI) model [11]. However, the LRI model does not include the NCX current.

In this paper, we use the Shannon model [12] which describes the detailed dynamics of intracellular calcium. Applying the bifurcation analysis method to this model, we aim to clarify the bifurcation mechanism [14] of generating LQTS. As a first step, we investigate what kinds of ionic currents affect the generation of QT prolongation in this study. As a result, we obtain that increasing the sodium-calcium exchange current or the L-type calcium current is a key to the generation of QT prolongation and EADs.

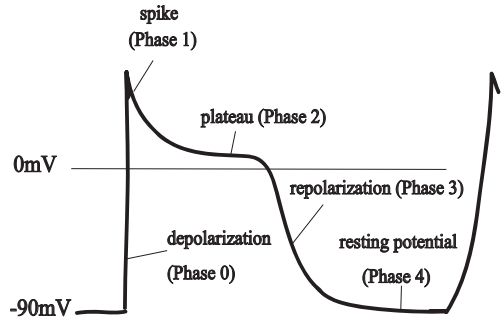

Figure 1: Cardiac action potential

2. Model

The Shannon model describes the detailed calcium dynamics in the rabbit ventricular myocyte. In this model, four compartments are considered: the sarcoplasmic reticulum (SR), the junctional cleft for SR, the subsarcolemmal space, and the bulk cytosolic space. The calcium dynamics is described by the L-type Ca channels, the Ca leak, the Ca pump, the NCX, and Ca buffering.

The membrane potential is given by

$$\begin{aligned} C\frac{dV}{dt} &= -(I_{Na} + I_{Nb} + I_{NaK} + I_{Kr} + I_{Ks} + \\ &\quad I_{tos} + I_{tof} + I_{K1} + I_{NaCa} + I_{ClCa} + \\ &\quad I_{Clb} + I_{CaL} + I_{Cab} + I_{Cap} + I_{syn}), \end{aligned} \tag{1}$$

where V is the membrane potential, C is the cell membrane capacitance, and I_j are ionic currents except for synaptic

current I_{syn}. All ionic currents in this model are shown in Tab 1. I_{syn} is given by

$$I_{syn} = G_{syn}(V - V_{syn})s(t^*), \tag{2}$$

where G_{syn} is the maximum synaptic conductance, V_{syn} is the reversal potential, and $s(t^*)$ is given by

$$s(t^*) = \frac{\tau_1}{\tau_2 - \tau_1}\left(-\exp\left(-\frac{t^*}{\tau_1}\right) + \exp\left(-\frac{t^*}{\tau_2}\right)\right), \tag{3}$$

where τ_1 and τ_2 are the raise and decay time of the synapse. We identify these values ($\tau_1 = 5.5$ and $\tau_2 = 90.0$[ms]) from the experimental data [13]. t^* is the time that is reset at every nT (n is a natural number, and T is the BCL: basic cycle length). We check the periodicity of the trajectory by using the state variables at every nT. The values of the parameters related with the synapse are fixed as $G_{syn} = 4.0$ and $V_{syn} = -29$.

Some ionic currents have the following form

$$I_j = G_j \cdot y \cdot (V - E_j),$$

where G_j is the maximum conductance and E_j is the reversal potentials for ion j. The gating variable y is given by

$$\frac{dy}{dt} = \frac{y_\infty - y}{\tau_y}$$

where τ_y and y_∞ are time constant and the value of y in the steady state, respectively. There are 14 gating variables in the Shannon model. The kind of state variables is shown in Tab 2. In total, the Shannon model is described by 39-dimensional ordinary differential equations.

Table 1: Ionic currents in Shannon model

Abbreviation	Ionic current
I_{Na}	fast Na current
I_{NaBk}	Na leas current
I_{NaK}	Na-K pump current
I_{CaL}	L-type Ca current
I_{CaB}	Ca leak current
I_{CaP}	Ca pump current
I_{NaCa}	Na-Ca exchange current
I_{ClCa}	Ca-dependent Cl current
I_{Kr}	rapidly activated K current
I_{Ks}	slowly activated K current
I_{tos}	slow transient outward K current
I_{tof}	fast transient outward K current
I_{K1}	inward rectifying K current
I_{Clb}	background SL CL current

Table 2: State variables

state variables	its number
membrane potential	1
Na concentrations	3
Ca concentrations	4
gate variables	14
channel states for ryanodine receptor	3
Na buffering	2
Ca buffering	12

3. Results

There are 14 ionic currents in the Shannon model. We investigate the influence of changing the value of each current (multiplying I_j by artificial parameter Z_j) on generation of QT prolongation and EADs. We study that the interval of external stimulus (BCL) equals 1000 [ms]. As a result, arrhythmia is observed when each of two ionic currents (sodium-calcium exchange current I_{NaCa} and L-type calcium channel current I_{CaL}) is changed. We calculate a two-parameter bifurcation diagram and clarify the dominant parameter for generating QT prolongation and EADs.

We show a two-parameter bifurcation diagram in Fig. 2. In this diagram, Z_{CaL} and Z_{NaCa} are artificial parameters of I_{CaL} and I_{NaCa}, respectively. The solid curves denoted by N and I indicate Neimark-Sacker and period-doubling bifurcations, respectively. In the region colored by gray, we observe a normal waveform of the membrane potential as shown in Fig. 3. The neuron fires at every $1000 \times n$ [ms], where n is a natural number. Here, 1000 means the period of the external stimulus. This normal state suddenly disappears by crossing the bifurcation curves.

To show responses after crossing the bifurcation, we use one-parameter bifurcation diagrams as shown in Fig. 4. Figures 4(a) and 4(b) are obtained by changing the parameter values along the arrows (a) and (b) in Fig. 2, respectively. The horizontal axis indicates the peaks of the membrane potential after transient time. We observe one point until $Z_{NaCa} \simeq 3.85$ and $Z_{CaL} \simeq 1.55$, which means the membrane potential of the cardiac muscle has one peak during one external stimulus. Roughly speaking, we also observe that the points are on three lines: the top ($V \simeq 33$), the middle ($V \simeq 0$), and the bottom ($V \simeq -35$). We show waveforms of V near bifurcation points in Figs. 5(a) and 5(b). The points on the bottom and middle in Fig. 4 indicate small and large peaks shown by the arrow in Figs. 5(a) and 5(b), respectively. Note that the appearance of the bottom points does not correspond to a bifurcation, it is just the transform of the waveform. On the other hand, the emergence of the middle points, which means the emergence of an EAD, corresponds to a bifurcation; the type of a bifurcation (Neimark-Sacker or period-doubling) depends on the parameter value. EADs occur with abnormal depolarization during phase 2 or phase 3, and are caused by an in-

crease in the frequency of abortive action potentials before normal repolarization is completed [15].

Figure 6 is obtained by changing the parameter values along the arrow (c) ($Z_{NaCa} = 2$) in Fig. 2. The horizontal axis is the same as that of Fig. 4. The Neimark-Sacker bifurcation occurs at $Z_{CaL} \simeq 2$, and EADs appear as shown in Fig. 7(a). We can see a plurality of projections and prolongation of the action potential duration (APD), which correspond to QT prolongation in the electrocardiogram. In Fig. 7(b) we show a membrane potential waveform in case of $Z_{NaCa} = 2$ and $Z_{CaL} = 3.5$. We can see the irregular wave. This membrane potential waveform is extremely dangerous.

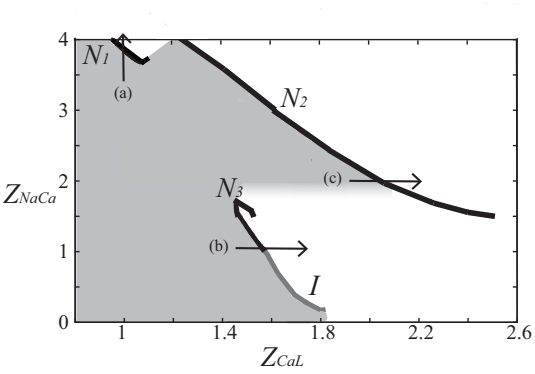

Figure 2: Two-parameter bifurcation diagram

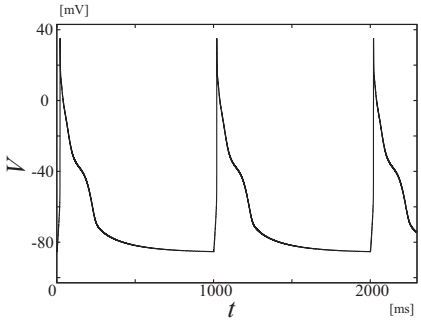

Figure 3: Waveform of membrane potential at normal parameter values ($Z_{CaL} = 1$, $Z_{NaCa} = 1$)

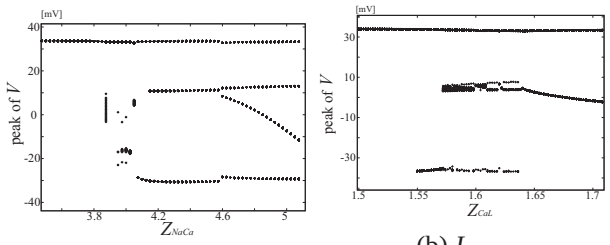

(a) I_{NaCa} (b) I_{CaL}

Figure 4: One-parameter bifurcation diagram for changing the value Z_j

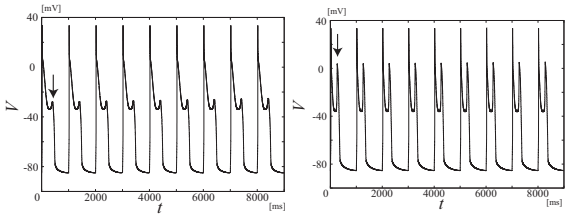

(a) $Z_{NaCa} = 3.85$ (b) $Z_{CaL} = 1.575$

Figure 5: Membrane potential waveforms

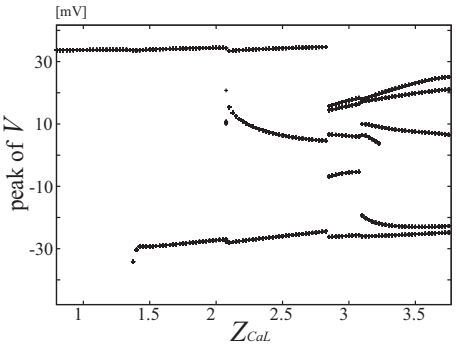

Figure 6: One-parameter bifurcation diagram for changing the value Z_{CaL}

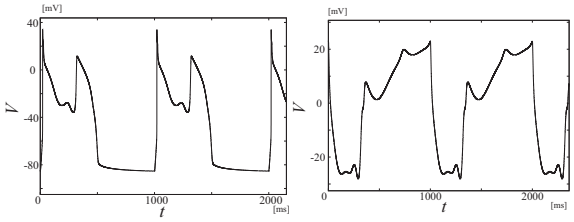

(a) $Z_{CaL} = 2.1$ (b) $Z_{CaL} = 3.5$

Figure 7: Waveforms of membrane potential for $Z_{NaCa} = 2$

4. Conclusion

In this study, we examined dependence of generating EADs and QT prolongation on parameter values in the Shannon mathematical model. We calculated a two-parameter bifurcation diagram. As a result, two ionic currents (sodium-calcium exchange current I_{NaCa} and L-type calcium channel current I_{CaL}) are keys to the generation of EADs and QT prolongation. We determined that a normal state becomes unstable by bifurcations. Before a bifurcation, the action potential duration (APD) becomes a little longer as the I_{NaCa} or I_{CaL} is increased. After a bifurcation, EADs suddenly appear as a stable state and at the same time the APD becomes very long which corresponds to QT prolongation. Extremely dangerous waveforms like ventricular fibrillation were obtained after occurrence of QT prolongation. This agrees with that QT prolongation is a sign of sudden cardiac cessation.

Acknowledgments

This work was supported by JSPS KAKENHI Grant Number 15K00405. We thank Prof. T. Yoshinaga of Tokushima University for providing his powerful bifurcation analysis tools.

References

[1] Guidelines for Diagnosis and Management of Patients with LongQT Syndrome and Brugada Syndrome, http://www.j-circ.or.jp/guideline/pdf/JCS2013_aonuma_h.pdf/2012/(in Japanese) .

[2] H. Henry and W.J. Rappel, The role of M cells and the long QT syndrome in cardiac arrhythmias: simulation studies of reentrant excitations using a detailed electrophysiological model, Chaos, 14(1), 172–182, 2004.

[3] R.H. Clayton, A. Bailey, V.N. Biktashev and A.V. Holden, Re-entrant cardiac arrhythmias in computational models of long QT myocardium, Journal of Theoretical Biology, 208(2), 215–225, 2001.

[4] T. Aiba et al., Cellular and ionic mechanism for drug-induced long QT syndrome and effectiveness of verapamil, J. American College of Cardiology, 45(2), 300–307, 2005.

[5] A. Parikh et al., Ranolazine stabilizes cardiac ryanodine receptors: a novel mechanism for the suppression of early afterdepolarization and torsades de pointes in long QT type 2, Heart Rhythm, 9(6), 953–960, 2012.

[6] H. Tanaka et al., Effect of SEA0400, a novel inhibitor of sodium calcium exchanger, on myocardial ionic currents, British Journal of Pharmacology, 135(5), 1096–1100, 2002.

[7] P. Milberg et al., Inhibition of the Na+/Ca2+ exchanger suppresses torsades de pointes in an intact heart model of long QT syndrome-2 and long QT syndrome-3, Heart Rhythm, 5(10), 1444–1452. 2008.

[8] D.M. Johnson et al., IKs restricts excessive beat-to-beat variability of repolarization during beta-adrenergic receptor stimulation, Journal of Molecular and Cellular Cardiology, 48(1), 122–130, 2010.

[9] M. Maruyama et al., Genesis of phase 3 early afterdepolarizations and triggered activity in acquired long-QT syndrome, Circulation: Arrhythmia and Electrophysiology, 4(1), 103–111, 2011.

[10] Z. Zhao et al., Revisiting the ionic mechanisms of early afterdepolarizations in cardiomyocytes: predominant by Ca waves or Ca currents?, American J. Physiology-Heart and Circulatory Physiology, 302(8), H1636–H1644, 2012.

[11] D.X. Tran et al, Bifurcation and chaos in a model of cardiac early afterdepolarizations. Physical Review Letters, 102(25), 258103, 2009.

[12] T. Shannon, F. Wang, J. Puglisi, C. Weber, D. Bers, A Mathematical Treatment of Integrated Ca Dynamics within the Ventricular Myocyte, Biophysical Journal, 3351–3371, Nov 2004.

[13] T. Yazawa, J. L. Wilkens, H.E.D.J. ter Keurs and M. J. Cavey, Structure and contractile properties of the ostial muscle (musculus orbicularis ostii) in the heart of the American lobster, J. Comp. Physiol. B, 169, 529–537, 1999.

[14] H. Kitajima, E. Ioka and T. Yazawa, Generation mechanism of alternans in Luo-Rudy model, Int. J. Bifurcation and Chaos, 26(5), 1650075, 2016.

[15] Afterdepolarizations may lead to cardiac arrhythmias, https://en.wikipedia.org/wiki/Afterdepolarization, 2016/7/26.